Scientific Research Publishing

Journal of Materials Science and Chemical Engineering, 2022, 10, 16-28
https://www.scirp.org/journal/msce
ISSN Online: 2327-6053
ISSN Print: 2327-6045

Features of the Conductivity of the $Ag_8Ge_{1-x}Mn_xTe_6$ Solid Solutions

Rashad Rahimov, Aynur Gahramanova, Durdana Arasly, Almaz Halilova, Ilgar Mammadov

Institute of Physics of Azerbaijan National Academy of Sciences, Baku, Azerbaijan
Email: rashad@physics.science.az, rashadrahim48@gmail.com

How to cite this paper: Rahimov, R., Gahramanova, A., Arasly, D., Halilova, A. and Mammadov, I. (2022) Features of the Conductivity of the $Ag_8Ge_{1-x}Mn_xTe_6$ Solid Solutions. *Journal of Materials Science and Chemical Engineering*, **10**, 16-28.
https://doi.org/10.4236/msce.2022.105002

Received: April 6, 2022
Accepted: May 17, 2022
Published: May 20, 2022

Abstract

Samples of $Ag_8Ge_{1-x}Mn_xTe_6$ solid solutions with different manganese content (x = 0, 0.05, 0.1, 0.2) were prepared by fusing and further pressing their powders under the pressure of 0.6 GPa. In addition of Mn atoms to the Ag_8GeTe_6 compound leads to compression of their lattice. All p-type samples acquire a high resistance below the transition at temperatures of 180 - 220 K. The electrical conductivity of all compositions in the range of 220 - 300 K increases due to hopping mechanism, and at temperatures T > 320 K, a semiconductor characteristic is observed. By studying impedance spectra of samples, it was established that at 80 K solid solutions behave like a homogeneous dielectric material. At high temperatures and frequencies of an external electric field, a significant role of grain boundaries in conductivity was revealed. The dielectric anomaly occurring at low frequencies is also associated with an effect that manifests itself in the grain boundary.

Keywords

Solid Solutions, X-Ray Diffraction, Hopping Conductivity, Electrical Conductivity, Impedance Spectra

1. Introduction

In recent decades, studies of ionic crystals have become widespread, which are used in many areas of electronics and energy. The devices used in this field are based on ion-conducting solid crystals. The study of ion transport processes in solids has led to the fact that the range of objects with ionic conductivity has significantly expanded, and ionic conductors have begun to be actively used in various devices used in electronics and power engineering. All of these devices contain solid crystalline or polymer ion conductors. The operation of all devices is based on electrochemical processes that occur at the electrode-ionic conductor

interface and in the polycrystalline electrolyte itself. One of the most accessible methods for studying electrochemical and electrophysical processes in ion-conducting materials is impedance spectroscopy, which is used as an informative working tool in various fields of electrochemistry, physics, and materials science. In recent years, approaches have been developed and scientifically substantiated that allow obtaining information both about the properties of the system under study and about the mechanism of the processes occurring in it. At present, the impedance technique in the study of materials is mainly used to determine the magnitude of ionic conductivity. For such measurements, the average frequency range is sufficient.

Ionically conductive Ag_8GeTe_6 ternary compound due to the complex crystal structure [1] [2] [3] and the large size of the unit cell, has many unusual properties: it exhibits low thermal conductivity and a small band gap (0.4 eV) [4], it is an example of a material with superionic conductivity and has a promising thermoelectric characteristics at 500 K and above. Since this compound as a perspective material for thermoelectricity can be used as a converter of thermal energy into electrical energy, and also as an electrolytic material for the accumulation of the electric energy in batteries, therefore in the last two decade there has been an increased interest in the study of this type of materials [4] [5] [6]. As known that by changing the composition of a solid solution, one can control its parameters and the temperature of the phase transitions that occur. Impurity atoms, which are part of the alloy, lead to violation of the potential field and periodicity in the crystal. A deformation region is formed around defects and impurity atoms, which distorts the crystal lattice. Such defects in ionic crystals further reduce the free path of phonons and charge carriers, that resulting significantly changes of physical properties. In this work, new alloys were obtained by adding highly soluble and diffusible manganese to the Ag_8GeTe_6 ternary compound. Mn atoms as a magnetic impurity cause strong lattice distortion and, consequently, change the transport of phonons and charge carriers. Early analysis showed that structures of the synthesized system have those of Ag_8GeTe_6 compound, however, reflex of the composition containing 10% manganese insignificantly shift towards small angles, *i.e.* introduction of manganese atoms leads to compressibility in the matrix lattice [7]. On the other hand, with the introduction of Mn atoms into Ag_8GeTe_6 alloys, weakly antiferromagnetic material is created [8]. In this article, the conductivity in a stable electric field and the impedance spectroscopy of the $Ag_8Ge_{1-x}Mn_xTe_6$ solid solution are studied.

2. Experimental

$Ag_8Ge_{1-x}Mn_xTe_6$ solid solutions with different manganese concentration (x = 0; 0.05; 0.1; 0.2) were synthesized in two stages. At the first stage, elements Ag, Ge, Te and Mn in a stoichiometric ratio were placed in an ampoule, then evacuated up to 1.3 mPa pressures and sealed. The ampoule was vibrated and gradually heated to 1250 K temperature, for 4 hours it was kept at this temperature and

then annealed at 900 K for 50 hours. In the second stage, the synthesized material was chopped in an agate mortar and sieved through a 100 micron sieve. Then by pressing its powder circular and parallelepiped shapes under the pressure of 0.6 GPa were obtained. Samples were homogenized at ~800 K temperature for 10 hour.

The XRD and differential scanning calorimetric analyzes were performed for the certification of samples. X-ray phase analysis of the samples was carried out on a Bruker D2 Phaser diffractometer at the angles between 5 and 80 degree using Cu K_α radiation. Calorimetric studies were performed in the 100 - 900 K temperature range in the scanning differential calorimeter (DSC) "NETZSCH DSC 204F1" (Germany) in an argon atmosphere. Sapphire was chosen as an etalon matter, the heating rate was 10 K/min and inert gas (argon) rate was 20 ml/min. Microstructural and elemental analysis was carried out on a SEM JEOL 6610 LV electron microscope equipped with EDX energy-dispersive X-ray spectroscopy.

Electrical conductivity was measured in the temperature range of 80 - 700 K using four probes method. To measure the specific conductivity at an alternating electrical field and at a frequency of 20 Hz to 1 MHz, samples were made in the form of a disk with 6 mm diameter and 1 mm thickness. A silver paste was applied to the sample plane, and then copper wires were attached to this layer. Contact resistance has been tested up to 1.0 V. Conductivity and capacitances, depending on the frequency of electric field, were measured on a Precision LCR Meter 1920 instrument (IET Labs). Real and imaginary parts of the dielectric constant were calculated from the measured capacitance and conductivity data.

3. Results and Discussion

Diffraction patterns for $Ag_8Ge_{1-x}Mn_xTe_6$ solid solution (x = 0; 0.1; 0.2) is shown in **Figure 1**. Analysis showed that the synthesized solutions have structures identical to Ag_8GeTe_6 ternary compound. However, compositions containing 10% and 20% manganese reflexes slightly shift towards the small angles, *i.e.* introduction of the manganese atoms leads to the compression of the lattice. As can be seen from **Figure 1** for $Ag_8Ge_{1-x}Mn_xTe_6$(x = 0.20) sample all reflexes are identical to the Ag_8GeTe_6 ternary compound, but weak reflections at the angles between 28.8 and 31.5 degrees correspond to the MnTe compound [9].

Note that in literature, information about the low-temperature structure of Ag_8GeTe_6 is ambiguous. Ag_8GeTe_6 belongs to the space group, and the lattice constant is a = 11.58 ± 0.02A [1]. In the argyrodite family of compounds undergoes multiphase structural transitions below room temperature. According to [10] four transitions were observed in the Ag_8GeTe_6 compound: at 223 K and 245 K, first-order (structural) transitions, and at 156 K and 170 K—second order. At the same time, some authors suggest that all transitions are either cubic ($F4\bar{3}m$) or pseudo-cubic (R3) and are associated with the ordering of Ag+ [11] [12] [13].

Our DSC results for $Ag_8Ge_{1-x}MnxTe_6$ samples at x = 0; 0.05; 0.1 and 0.2 are presented in **Figure 2**. As seen in Ag_8GeTe_6 endothermic peaks at 225 K, 243 K

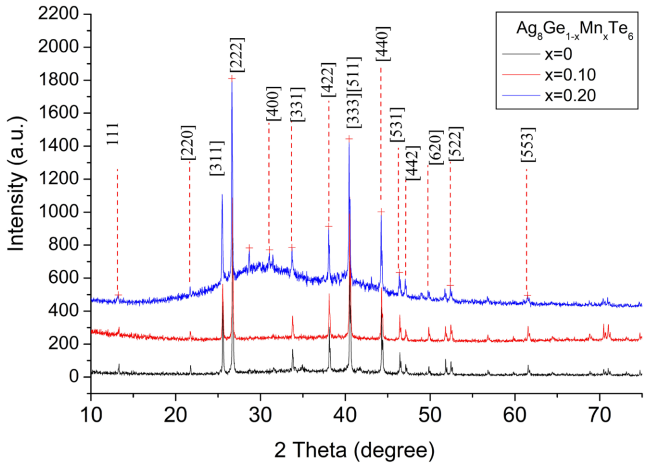

Figure 1. XRD patterns of the $Ag_8Ge_{1-x}Mn_xTe_6$ solid solutions.

and 638 K are observed. Same two endothermic peaks below room temperature are observed in $Ag_8Ge_{1-x}Mn_xTe_6$ solutions, but above the room temperature observed addition peaks at ~340 K and at 626 K.

As shown from **Figure 3**, the elemental analyzes performed on a SEM JEOL 6610LV microscope correspond to the composition of the solid solution.

Electrical conductivity measurements for $Ag_8Ge_{1-x}Mn_xTe_6$ alloys (x = 0; 0.05; 0.1 and 0.2) at the static electrical field in the 100 - 650 K temperature range have been carried out and shown in **Figure 4**.

All samples have high-resistivity at T < 180 K temperatures. In the temperature range 200 - 650 K, conductivity of all samples is of an activation character, and their value increases by almost two or three orders of magnitude. Note that in the temperature range of 180 - 300 K, conductivity is hopping character. According to Mott's theory [14], electrical conduction occurs by a hopping mechanism from a localized state located in a narrow energy band close to the Fermi level. Transport through localized states occurs as a result of hopping of charge carriers from one localized center to another. Hopping conduction occurs in compensated semiconductors during the transition between the nearest neighboring centers at low temperatures. With weak compensation of donors in the impurity band, the energy dependence of the density of states passes through a maximum. This occurs at the ionization energy of the maximum isolated donor. When the initial and final hopping centers are close, they have energies close to the maximum density of states. For the jump to take place, the next center must be empty. The hopping conductivity is highly dependent on the concentration of impurities and such a change is usually described as an exponential dependence. It is note, that the exponential dependence of the conductivity on the impurities concentration is the main experimental evidence for the hopping conductivity. As follow we were analyzed the temperature dependences of conductivity $\sigma(T)$ in the temperature range 220 - 300 K using the Mott relation [14] [15].

$$\sigma(T) = \sigma_0 \exp\left[-\left(\frac{T_0}{T}\right)^{1/4}\right], \quad (1)$$

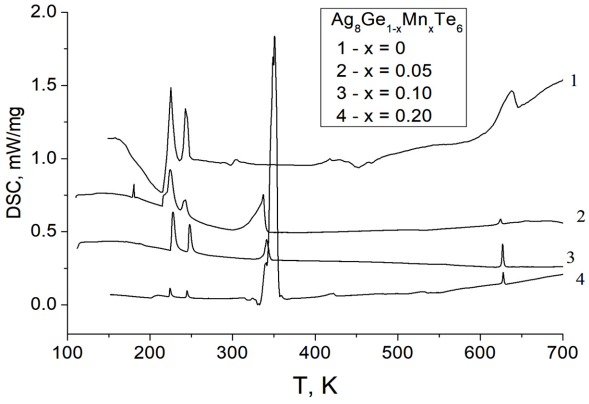

Figure 2. Results of DSC analyze for $Ag_8Ge_{1-x}Mn_xTe_6$ solid solutions.

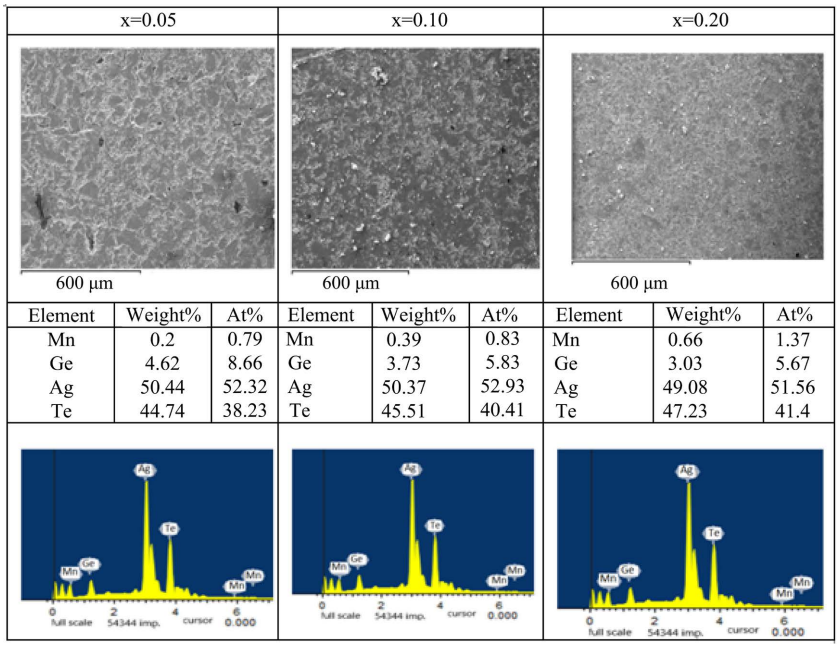

x=0.05			x=0.10			x=0.20		
Element	Weight%	At%	Element	Weight%	At%	Element	Weight%	At%
Mn	0.2	0.79	Mn	0.39	0.83	Mn	0.66	1.37
Ge	4.62	8.66	Ge	3.73	5.83	Ge	3.03	5.67
Ag	50.44	52.32	Ag	50.37	52.93	Ag	49.08	51.56
Te	44.74	38.23	Te	45.51	40.41	Te	47.23	41.4

Figure 3. Elemental analyzes for $Ag_8Ge_{1-x}Mn_xTe_6$ alloys (x = 0.05; 0.1 and 0.2).

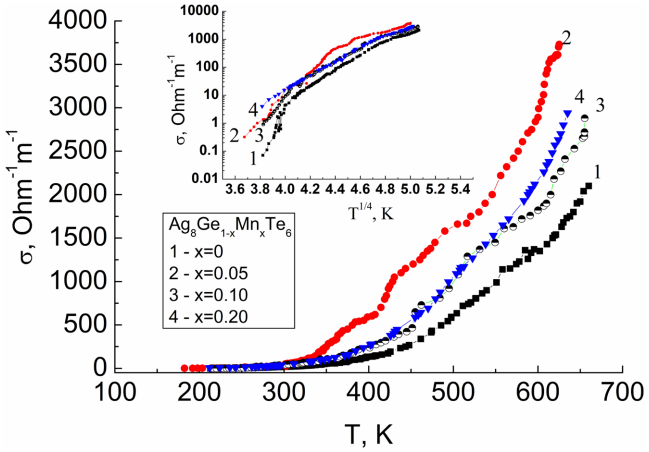

Figure 4. Temperature dependence conductivity of $Ag_8Ge_{1-x}Mn_xTe_6$ solid solutions (in the insert the dependence $\ln\sigma\left(T^{1/4}\right)$.

where $T_0 = \beta / g(\mu) r^3 k_B$, $g(\mu)$ is the Fermi level density of localized states, r is the radius of localized states near the Fermi level, k_B is Boltzmann's constant, and β depends on the dimensionality of the system ($\beta = 21$ in three dimensions [16]). The data were found to give linear Mott plots in a certain temperature range. This leads us to assume that, in this temperature range, charge transport in these materials is due to the hopping of charge carriers between localized states in a narrow energy band near the Fermi level. Structural disorder, interstitial impurities, vacancies, and dislocations distort crystal structure periodicity, producing localized states with energies falling in the band gap of a perfect crystal. As can be seen from **Figure 4**, at a temperature range of 220 - 300 K, for Ag_8GeTe_6 the Mott dependence (1) is fulfilled. The value of T_0 is determined by the inclination of the line in the coordinates $\ln\sigma\left(T^{1/4}\right)$:

$$T_0^{1/4} = \frac{\ln\sigma_1 - \ln\sigma_2}{T_1^{1/4} - T_2^{1/4}} \tag{2}$$

Using the present experimental data, we calculated density of the localized states for $Ag_8Ge_{1-x}Mn_xTe_6$: $g(\mu) = 1.378 \times 10^{18}$ eV^{-1} cm^{-3} (for x = 0); $g(\mu) = 1.684 \times 10^{19}$ eV^{-1} cm^{-3} (for x = 0.05); $g(\mu) = 6.381 \times 10^{18}$ eV^{-1} cm^{-3} (for x = 0.1) and $g(\mu) = 4.06 \times 10^{19}$ eV^{-1} cm^{-3} (for x = 0.2). This leads us to assume that, in this temperature range, charge transport in these materials is due to the hopping of charge carriers between localized states in a narrow energy band near the Fermi level.

Since the studied samples are granular, because the boundary between the grains well be plays a significant role in the hopping mechanism. Calculations that were made using the Debye-Scherer model showed that the grain size in the studied solutions is approximately 1.5 μm. Therefore charges can form in the intergranular boundaries and they significantly affect conductivity and change dielectric constant of the material. The effect of grain boundaries on conductivity can be determined by conducting an experiment with an alternating electric field. Using impedance spectroscopy information can be obtained on carrier transport in a sample taking into account its microstructure, transport features in layered structures [17] and phase transitions in ionic crystals [18], effect of impurity on electrophysical properties in the doped materials [19], as well as the role of crystallites and their interfaces in the conductivity of crystal [20].

The dependences of the dielectric permittivity of $Ag_8Ge_{1-x}Mn_xTe_6$ solid solutions (x = 0; 0.05; 0.1 and 0.2) at 80 K and 300 K temperatures, calculated on the basis of the experimental data of conductivity and capacitance depending on the frequency of the electric field, are shown in **Figure 5**. A sample with a composition of 5% manganese at 80 K has a maximum value of ε equal to 40 at a frequency of 20 Hz and decreases to 30 at a frequency of 2×10^5 Hz. At 300 K temperature, these values increase anomalously. The sharp increase in the permittivity ε is due to the fact that the concentration of ionic charge carriers increases with an increase in temperature.

Figure 6 show the results of the real (Z') and imaginary parts (Z'') of the impedance of $Ag_8Ge_{1-x}Mn_xTe_6$ (x = 0; 0.05; 0.1 and 0.2) solid solutions at 80 K and

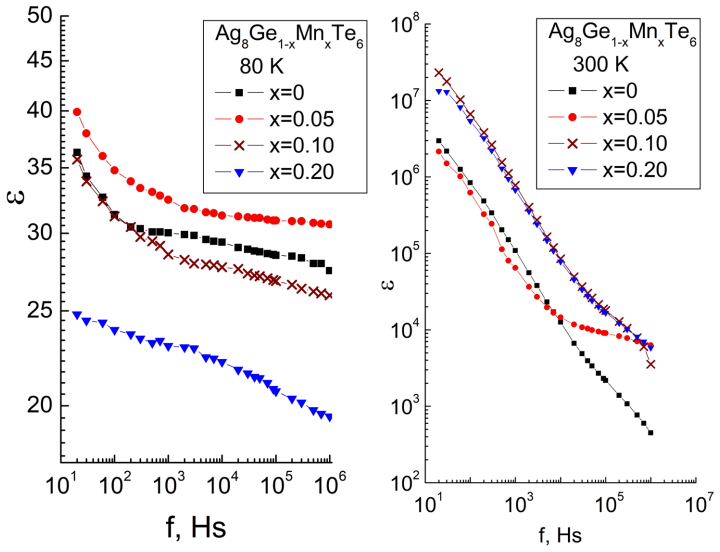

Figure 5. The dependences of the dielectric permittivity of $Ag_8Ge_{1-x}Mn_xTe_6$ solid solutions at 80 K and 300 K temperatures.

300 K temperatures. As can be seen, at 80 K the $Z'(f)$ dependence decreases stronger (from 10^9 Ohm to 100 Ohm) than the $Z''(f)$ dependence (from 10^9 Ohm to 10^4 Ohm). At 300 K temperature $Z'(f)$ dependence up to a frequency of 10^5 Hz changes very slowly, and above frequencies of 10^5 Hz it begins to decrease. For the x = 0.05 composition $Z'(f)$ dependence is more stronger. The dependence of $Z''(f)$, on the contrary, increases with frequency. At this temperature, $Z''(f)$ dependence is stronger than the $Z'(f)$ dependence and their ratio changes from hundred to one with an increasing frequency.

In order to obtain information on the mechanism of the formation of polarization, analysis of the impedance spectra (hodographs—dependence of Z'' on Z') for these solid solutions was carried out. In **Figure 7** hodographs were carried out at 80 K and 300 K temperatures. As seen at 80 K temperature the hodograph passes through the origin of the coordinate and forms an arc. The arcs radii for different compositions are different: for the composition x = 0.1 is the smallest, and for x = 0.2 is the largest. This type of hodograph indicates that at 80 K temperature the alloys are homogeneous. At 300 K temperature two arcs of circles are observed in the hodograph, the centers of which are shifted from the Z' axis and with an increasing composition approaching the origin of coordinates. It should be noted that in this frequency range no kind of lattice polarization can take place. As a rule, high-frequency arc is associated with transport within the grain volume, and the arc corresponding to lower frequencies reflects the contribution of the intercrystalline boundary [19]. An equivalent circuit of such a spectrum is a parallel RC-circuit.

The dielectric anomaly that occurs at low frequencies is associated with an effect that manifests in the intergranular boundary [21]. The charges are formed in the intergrain boundary and they change the dielectric constant of the material. According to the authors [22] at low temperatures, the dominant part of the

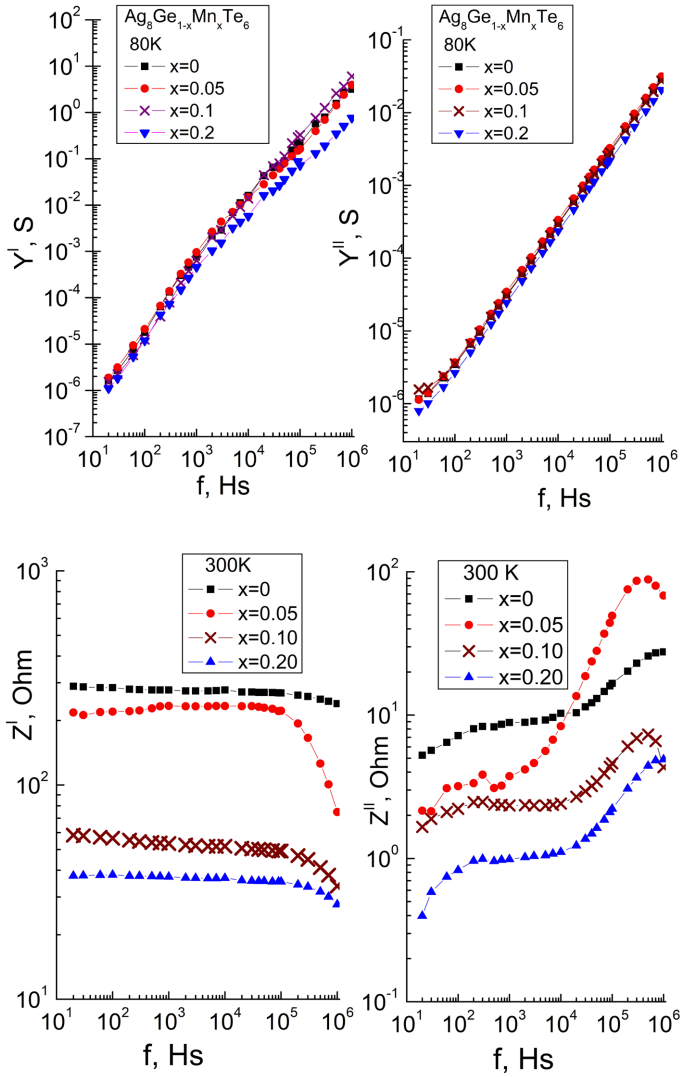

Figure 6. Frequency dependencies of the real Z^{I} and imaginary parts Z^{II} of the impedance at 80 K and 300 K for $Ag_8Ge_{1-x}Mn_xTe_6$ solid solutions.

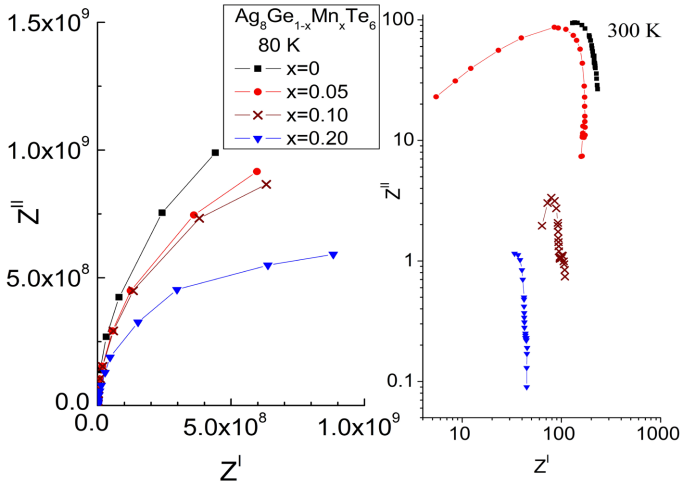

Figure 7. The hodograph at 80 K and 300 K for $Ag_8Ge_{1-x}Mn_xTe_6$ solid solutions.

defects is in the neutral charge state. With an increasing temperature the jump charge exchange between defects can begin. The defect may be in the charge state, and after some time it returns to the neutral state. Thus hopping charged defects that introduce deep levels into the forbidden zone should lead to the increase of dielectric constant in the external electric field.

To detect boundary (interfacial) polarization in heterogeneous systems, where dielectric constant at low frequencies can reach values of more than 1000, concept of "electrical module" is used [23]. To relate the features that were found in the impedance spectrum to the capacitance, "electrical module" is defined by the following standard formulas:

$$Y = \frac{1}{Z^I(f) + iZ^{II}(f)} = \frac{Z^{II}}{Z^2} - i\frac{Z^{II}}{Z^2} = Y^I(f) - iY^{II}(f) \tag{3}$$

$$Y^{II} = \sim \omega C_{ef} \tag{4}$$

The results of calculations by the Equations (3) and (4) shown in **Figure 8**. The real and imaginary parts of the complex conductivity at 80 K vary with frequency by the ratio of $Y^I \sim f^{0.96}$. This shows that the calculated C_{ef} values according to the formula (4) are very weakly dependent on the frequency.

As seen from **Figure 9** for solid solutions of $Ag_8Ge_{1-x}Mn_xTe_6$ (x = 0; 0.05; 0.10) the reduced capacitance C_{ef}/C_0 (where $C_0 = \varepsilon_0 S/d$—is the geometric capacitance of the sample, ε_0—is the absolute dielectric constant, S is the contact area, d is the distance between contact) at 80 K and at low frequencies has values between of 27 to 38. At f > 500 Hs frequencies the effective capacitance for all compositions remains stable. This shows that at 80K solid solution behaves like a homogeneous dielectric material. Indeed, in homogeneous systems, parameter C_{ef} is equal to the capacitance C of a flat capacitor with dielectric constant ε. At 300 K temperature and low frequencies C_{ef}/C_0 ratio is approximately 10^7 and with increasing frequencies it decreases by three or four orders of magnitude, but only for x = 0.05 composition at frequencies f > 20,000 Hs remains stable.

It is important to highlight that the decrease of capacitance with the decrease of frequency is often detected. In this case, low-frequency effective value of the capacitance is abnormally high and the recalculated value (C_{ef}/C_0) exceeds 10^3 - 10^4. At the frequencies below 10^{12} Hz such phenomena cannot be caused by known types of polarization: ionic, electronic and orientation which is associated with fast electronic processes. As shown in [24] at the absence of dipole moments due to the characteristics of crystal lattice, an anomalously high effective capacitance connected with the sample inhomogeneity may be observed. Therefore, C_{ef}/C_0 parameter calculated by formula (3) for a given temperature range will be large enough and strongly dependent on frequency. Compared to the practically unchanged parameter Y^I, described capacitance decreases with an increasing frequency and approaches the value ε. Under the alternating electric field in the electronic subsystems between the crystallites reloading occurs gradually and this creates additional capacity at low frequencies. With an increase of external

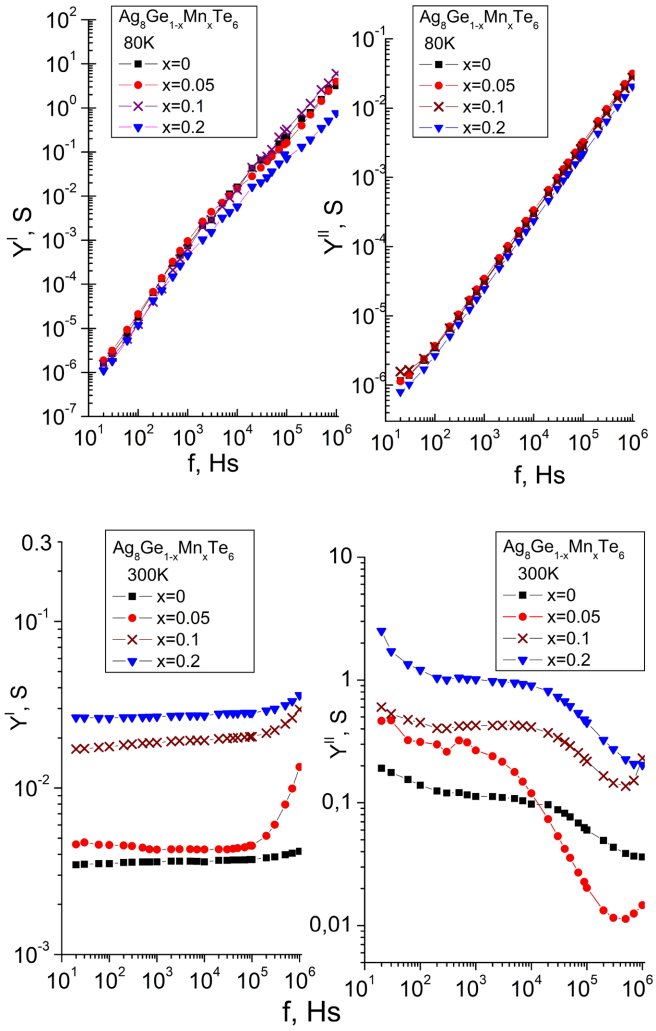

Figure 8. The real Y' and imaginary parts Y'' of the complex conductivity at 80 K and 300 K for $Ag_8Ge_{1-x}Mn_xTe_6$ solid solutions.

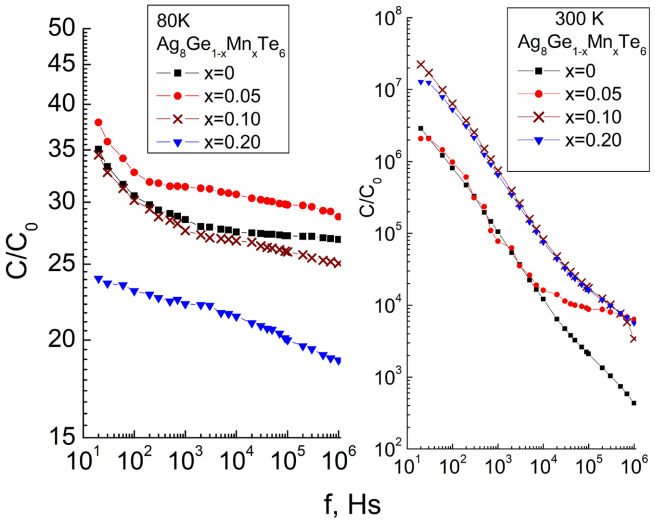

Figure 9. Frequency dependencies of the specific capacitance (C_{el}/C_0) at 80 K and 300 K for $Ag_8Ge_{1-x}Mn_xTe_6$ samples.

field frequency this contribution gradually disappears and a limit of the high-frequency capacitance approaches dielectric constant of the material. Described phenomena in the literature are called Maxwell-Wagner effects. In case of polycrystals this type of effects can take place as a result of polarization processes in the intercrystalline region [25] [26]. With an increase in frequency of the external field, this contribution gradually disappears and a limit of the high-frequency capacitance approaches dielectric constant of the material. In case of polycrystals, effects of this type can occur as a result of polarization processes in the intercrystalline region. As the frequency of external field increases, the slowest processes of repolarization of structurally inhomogeneous regions "freeze". The greater the frequency, the smaller the contribution to the integral value of capacitance, caused by the change in polarity of the external field of relaxation processes with the participation of carriers near the structural inhomogeneity.

4. Conclusions

Based on XRD study and using of differential scanning calorimeter (DSC) the structural identity of $Ag_8Ge_{1-x}Mn_xTe_6$ solid solution (x = 0, 0.05, 0.1, 0.2) with the Ag_8GeTe_6 ternary compound has been shown. Analysis of the impedance spectrum showed that at the temperature of liquid nitrogen complex conductivity increases with the external electric field frequency as $Y' \sim f^{0.96}$.

Reduced capacitance at 80 K temperature and at $f > 100$ Hs frequencies remains almost stable. This indicates that at low temperatures solid solution behaves like a homogeneous dielectric material. At room temperature reduced capacitance has abnormally high values at low frequencies and with increasing frequency decreases by three or four orders of magnitude. Complex conductivity at room temperature up to 10^5 Hz frequency remains constant, and increases at $f > 10^5$ Hz. This is related to the significant role of intergrain boundaries in the conductivity and dielectric constant.

Acknowledgements

The work was carried out within the framework of the science development program of the Azerbaijan National Academy of Sciences in 2020-2025.

Conflicts of Interest

The authors declare no conflicts of interest regarding the publication of this paper.

References

[1] Bendorius, R., Irzikevicius, A., Kindurys, A. and Tsvetkova, E.V. (1975) The Absorption Spectra of $Ag_8M^{IV}Se_6$ and $Ag_8GeX_6^{VI}$ Compounds. *Physica Status Solidi A*, **28**, K125-K127. https://doi.org/10.1002/pssa.2210280245

[2] Rysanek, N., Laruelle, P. and Katty, A. (1976) Structure Cristalline de Ag_8GeTe_6 (γ). *Acta Crystallografica Section B*, **32**, 692-696. https://doi.org/10.1107/S0567740876003804

https://journals.iucr.org/b/issues/1976/03/00/a13192/a13192.pdf

[3] Geller, S. (1979) The Crystal Structure of γ Ag_8GeTe_6, a Potential Mixed Electronic-Ionic Conductor. *Zeitschriftfür Kristallographie*, **149**, 31-47. https://doi.org/10.1524/zkri.1979.149.1-2.31

[4] Fujikane, M., Kurosaki, K., Muta, H. and Yamanaka, S. (2005) Thermoelectric Properties of Ag_8GeTe_6. *Journal of Alloys and Compounds*, **396**, 280-282. https://doi.org/10.1016/j.jallcom.2004.12.038

[5] Charoenphakdee, A., Kurosaki, K., Muta, H., Uno, M. and Yamanaka, S. (2008) Reinvestigation of the Thermoelectric Properties of Ag_8GeTe_6. *Physica Status Solidi* (*RRL*)—*Rapid Research Letters*, **2**, 65-67. https://doi.org/10.1002/pssr.200701302 https://onlinelibrary.wiley.com/doi/pdf/10.1002/pssr.200701302

[6] Zhu, T.J., Zhang, S.N., Yang, S.H. and Zhao, X.B. (2010) Improved Thermoelectric Figure of Merit of Self-Doped $Ag_{8-x}GeTe_6$ Compounds with Glass-Like Thermal Conductivity. *Physica Status Solidi* (*RRL*)—*Rapid Research Letters*, **4**, 317-319. https://doi.org/10.1002/pssr.201004278

[7] Gahramanova, A., Qasymov, V., Khalilova, A. and Rahimov, R. (2018) Thermodynamic Properties of $Ag_8Ge_{1-x}Mn_xTe_6$ Alloys. 7*th Rostocker International Conference*: "*Thermophysical Properties for Technical Thermodynamics*", Rostock, 26-27 July 2018, 73-74. https://www.ltt.uni-rostock.de/storages/uni-rostock/Alle_MSF/LTT/Thermam/Abstract_Book_THERMAM_2018.pdf

[8] Rahimov, R., Yanushkevich, K., Khalilova, A., Gahramanova, A., Mammadov, I., Arasly, D., Jivulko, A., Mitsiuk, V. and Rimskiy, G. (2021) Specific Magnetization and Magnetic Susceptibility $Ag_8Ge_{0.8}Mn_{0.2}Te_6$. 10*th Rostocker International Conference*: "*Thermophysical Properties for Technical Thermodynamics*", Rostock, 9-10 September, 143. https://www.ltt.uni-rostock.de/storages/uni-rostock/Alle_MSF/LTT/Thermam/Abstract_Book_THERMAM_2021.pdf

[9] Szwacki, N.G., Przezdziecka, E., Dynowska, E., Bogus, Ã.P. and Kossut, J. (2004) Structural Properties of MnTe, ZnTe, and ZnMnTe. *Acta Physica Polonica A*, **106**, 233-238. https://doi.org/10.12693/APhysPolA.106.233 http://przyrbwn.icm.edu.pl/APP/PDF/106/a106z210.pdf

[10] Kawaji, H. and Atake, T. (1994) Heat Capacity Measurement and Thermodynamic Study of Ag_8GeT_{e6}. *Solid State Ionics*, **70-71**, 518-521. https://doi.org/10.1016/0167-2738(94)90364-6

[11] Evain, M., Gaudin, E., Boucher, F., Petricek, V. and Taulellec, F. (1998) Structures and Phase Transitions of the A_7PSe_6 (A = Ag, Cu) Argyrodite-Type Ionic Conductors. I. Ag_7PSe_6. *Acta Crystallografica Section B*, **54**, 376-383. https://doi.org/10.1107/S0108768197019654

[12] Gaudin, E., Boucher, F., Petricek, V., Taulellec, F. and Evain, M. (2000) Structures and Phase Transitions of the A_7PSe_6 (A = Ag, Cu) Argyrodite-Type Ionic Conductors. II. β- and γ-Cu_7PSe_6. *Acta Crystallografica Section B*, **56**, 402-408. https://doi.org/10.1107/S0108768199016614 https://journals.iucr.org/b/issues/2000/03/00/lc0017/lc0017.pdf

[13] Gaudin, E., Boucher, F., Petricek, V., Taulellec, F. and Evain, M. (2000) Structures and Phase Transitions of the A_7PSe_6 (A = Ag, Cu) Argyrodite-Type Ionic Conductors. III. *α*-Cu_7PSe_6. *Acta Crystallografica Section B*, **56**, 972-979. https://doi.org/10.1107/S0108768100010260

[14] Mott, N.F. (1969) Conduction in Non-Crystalline Materials. *The Philosophical Maga-*

zine, **19**, 835-852. https://doi.org/10.1080/14786436908216338

[15] Fateev, M.P. (2010) Theory of Hopping Transfer in Disordered Systems. *Physics of the Solid State*, **52**, 1123-1130. https://doi.org/10.1134/S106378341006003X https://link.springer.com/article/10.1134/S106378341006003X

[16] Ragimov, S.S., Saddinova, A.A., Alieva, A.I., Selim-Zade, R.I. (2020) Hopping Conduction in $AgSbSe_2$ and $(AgSbSe_2)_{0.9}(PbTe)_{0.1}$. *Inorganic Materials*, **56**, 779-784. https://doi.org/10.1134/S0020168520080130

[17] Sardarly, R.M., Samedov, O.A., Alieva, N.A., Abdullayev, A.P., Huseynov, E.K., Hasanov, I.S. and Salmanov, F.T. (2014) On the Polarization Caused by Bulk Charges and the Ionic Conductivity in $TlInSe_2$ Crystals. *Semiconductors*, **48**, 427-431. https://doi.org/10.1134/S1063782614040253

[18] Alekperov, O., Samedov, O., Paucar, R., Abdulzade, N., Nakhmedov, E., Nadjafov, A., Wakita, K. and Mamedov, N. (2015) Impedance Spectroscopy Study of Phase Transitions to Ionic and Superionic Conductivity States in Ag_2S and Ag_2Se. *Physica Status Solidi C*, **12**, 610-614. https://doi.org/10.1002/pssc.201400366

[19] Joshi, M.J. (2017) Importance of Impedance Spectroscopy Technique in Materials Characterization: A Brief Review 47. *Mechanics, Materials Science & Engineering*, **9**. https://hal.archives-ouvertes.fr/hal-01504661/document

[20] Yakimchuk, A.V., Zaikina, J.V., Reshetova, L.N., Ryabova, L.I., Khokhlov, D.R. and Shevelkov, A.V. (2007) Impedance of $Sn_{24}P_{19.3}Br_xI_{8-x}$ Semiconducting Clathrates. *Low Temperature Physics*, **33**, 276-279. https://doi.org/10.1063/1.2719967

[21] Irvine, J.T.S., Sinclair, D.C. and West, A.R. (1990) Electroceramics: Characterization by Impedance Spectroscopy. *Advanced Materials*, **2**, 132-138. https://doi.org/10.1002/adma.19900020304 http://jtsigroup.wp.st-andrews.ac.uk/files/2015/06/Irvine_et_al-1990-Advanced_Materials.pdf

[22] Zukovskiy, P.W., Rodzik, A. and Shostak, Yu.A. (1997) Dielectric Constant and ac Conductivity of Semi-Insulating $Cd_{1-x}Mn_xTe$. *Semiconductors*, **31**, 610-614.

[23] Kudryashov, M. A., Mashin, A. I., Logunov, A. A., Chidichimo, G. and De Filpo, G. (2014) Dielectric Properties of Ag/PAN Nanocomposites. *Technical Physics*, **59**, 1012-1016. https://doi.org/10.1134/S1063784214070147

[24] Lunkenheimer, P., Bobnar, V., Pronin, A.V., Ritus, A.I., Volkov, A.A. and Loidl, A. (2002) Origin of Apparent Colossal Dielectric Constants. *Physical Review B*, **66**, Article ID: 052105. https://doi.org/10.1103/PhysRevB.66.052105

[25] Adams, T.B., Sinclair, D.C. and West, A.R. (2006) Characterization of Grain Boundary Impedances in Fine and Coarse-Grained $CaCu_3Ti_4O_{12}$ Ceramics. *Physical Review B*, **73**, Article ID: 094124. https://doi.org/10.1103/PhysRevB.73.094124

[26] Jana, P.K., Sarkar, S. and Chaudhuri, B.K. (2007) Maxwell-Wagner Polarization Mechanism in Potassium and Titanium Doped Nickel Oxide Showing Giant Dielectric Permittivity. *Journal of Physics D: Applied Physics*, **40**, 556-560. https://doi.org/10.1088/0022-3727/40/2/033